

Measurements of Stratospheric Water Vapor at Mauna Loa and the Effect of the Hunga Tonga Eruption

Gerald E. Nedoluha¹, R. Michael Gomez¹, Ian Boyd², Helen Neal², Douglas Ray Allen³, Alyn Lambert⁴, and Nathaniel J Livesey⁵

¹Naval Research Laboratory

²Bryan Scientific Consulting

³Naval Research Lab

⁴Jet Propulsion Lab (NASA)

⁵Jet Propulsion Laboratory

December 7, 2022

Abstract

The eruption of Hunga Tonga in January 2022 injected an amount of water vapor into the stratosphere that is unprecedented in the satellite era. In the ensuing months Aura Microwave Limb Sounder (MLS) measurements showed that this plume of water vapor spread from its original injection site at 20.50S to Mauna Loa, Hawaii at 19.50N, where an increase was observed in April by the ground-based Water Vapor Millimeter-wave Spectrometer (WVMS) instruments. Interannual variations in water vapor occur over Mauna Loa due to both dynamical variations in the tropical stratosphere and variations in the amount of water vapor crossing the tropical tropopause, and we place the observed stratospheric water vapor increase from Hunga Tonga into context of these other variations that have been observed since 2013.

1 **Measurements of Stratospheric Water Vapor at Mauna Loa and the Effect of the**
2 **Hunga Tonga Eruption**

3
4 **¹Gerald E. Nedoluha, ¹R. Michael Gomez, ²Ian Boyd, ²Helen Neal, ¹Douglas R. Allen, ³Alyn Lambert, and ³Nathaniel J. Livesey**

5
6 ¹Naval Research Laboratory, Washington, DC, USA

7 ²Bryan Scientific Consulting LLC, Charlottesville, VA, USA

8 ³Jet Propulsion Laboratory, California Institute of Technology, Pasadena, CA, USA

9 Corresponding author: Gerald Nedoluha (nedoluha@nrl.navy.mil)

10
11 **Key Points:**

12 A Aura MLS measurements showed that water vapor from the Hunga Tonga eruption spread to
13 20°N in April 2022

14 B Ground-based instruments at Mauna Loa observed an increase in the lower stratosphere in
15 April 2022.

16 C The April 2022 increase in water vapor in the upper stratosphere over Mauna Loa is placed in
17 context of interannual variations since 2013.

18
19
20 **Abstract**

21 The eruption of Hunga Tonga in January 2022 injected an amount of water vapor into the
22 stratosphere that is unprecedented in the satellite era. In the ensuing months Aura Microwave
23 Limb Sounder (MLS) measurements showed that this plume of water vapor spread from its
24 original injection site at 20.5°S to Mauna Loa, Hawaii at 19.5°N, where an increase was observed
25 in April by the ground-based Water Vapor Millimeter-wave Spectrometer (WVMS) instruments.
26 Interannual variations in water vapor occur over Mauna Loa due to both dynamical variations in
27 the tropical stratosphere and variations in the amount of water vapor crossing the tropical
28 tropopause, and we place the observed stratospheric water vapor increase from Hunga Tonga into
29 context of these other variations that have been observed since 2013.

30 **Plain Language Summary**

31 The eruption of the undersea Hunga Tonga volcano on 15 January 2022 injected large amounts of
32 water vapor into the stratosphere, breaking all records for direct injection of water vapor in the
33 satellite era. During the ensuing months this plume of water vapor spread from the original
34 injection site at 20°S to cover much of the Southern Hemisphere and reached as far as 20°N, where
35 it was first observed by a ground-based microwave instrument at Mauna Loa, Hawaii in April
36 2022. These ground-based measurements capable of detecting water vapor at the altitude of the
37 plume have been made since 2013, and we compare the sudden increase in water vapor caused by
38 the arrival of this plume over Mauna Loa with other variations that have occurred over the last
39 decade. This study lays the ground-work for an understanding of the effect of the water vapor
40 injected by the eruption on overall water vapor in the stratosphere in the coming years.

42 **1 Introduction**

43 The eruption of Hunga Tonga on 15 January 2022 injected large amounts of water vapor into the
44 stratosphere, breaking all records for direct injection of water vapor, by a volcano or otherwise, in
45 the satellite era [Millan et al, 2022]. The Hunga Tonga is an undersea volcano located at 20.5°S,
46 184.6°E, and Aura MLS measured water vapor anomalies at altitudes as high as 57 km. While the
47 direct injection of water vapor to 57 km was an impressive event, the injection of a much larger
48 amount of water vapor into the stratosphere (~10-50 km) is likely to have a much more long-lasting
49 effect on water vapor in the middle atmosphere.

50 Ground-based microwave measurements have been made at the Network for the Detection of
51 Atmospheric Composition (NDACC) site at Mauna Loa, Hawaii (19.5°N, 204.4°E) since 1996 by
52 a Water Vapor Millimeter-wave Spectrometer (WVMS) instrument [Nedoluha et al., 2022]. The
53 WVMS instruments are designed primarily for mesospheric (~50-80 km) H₂O measurements, but
54 no significant increase in mesospheric water vapor was detected by the WVMS instruments that
55 could be attributed to Hunga Tonga. While these instruments are focused on mesospheric trend
56 detection, they can be used to measure changes in water vapor in the stratosphere [Nedoluha et al.,
57 2011]. The water vapor injected into the lower and mid- stratosphere (~100-5 hPa, ~10-35 km) by
58 Hunga Tonga represents a unique opportunity to test the ability of the WVMS measurements to
59 detect unusual changes in water vapor in the mid-stratosphere (~10 hPa, ~30 km).

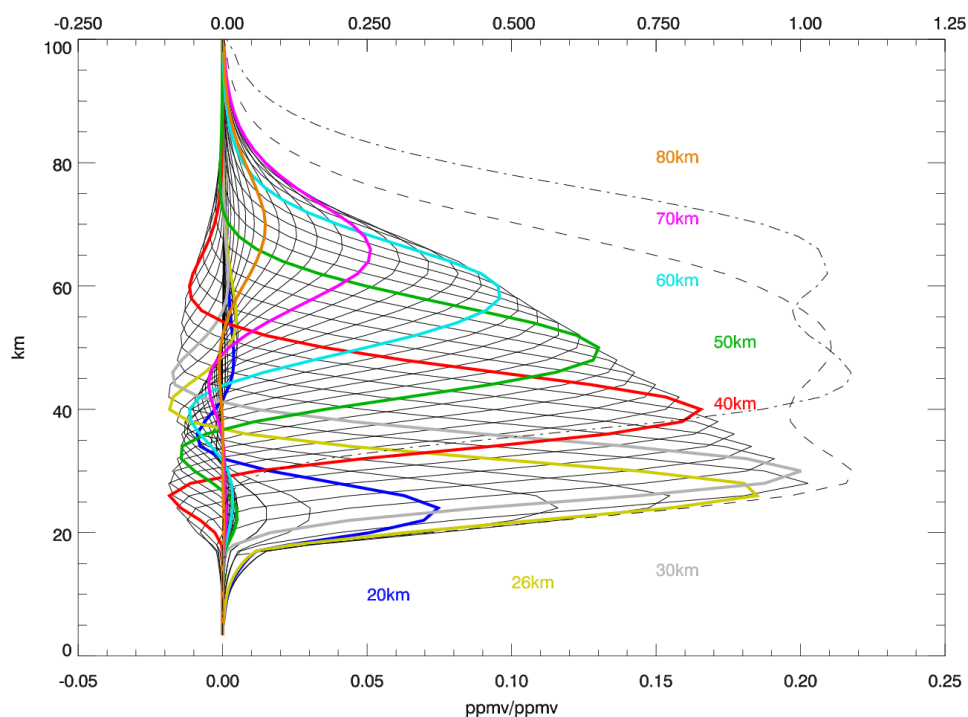
60 **2. Ground-based microwave measurements in the stratosphere**

61 The vertical profile of the water vapor measurements is obtained by measuring near the H₂O
62 emission peak at 22 GHz and making use of the change in pressure broadening with altitude.
63 Retrieving water vapor mixing ratios in the lower stratosphere requires a much broader spectral
64 measurement than is required in the mesosphere. A downward extension of the useful
65 measurement range into the lower stratosphere was accomplished by reducing instrumental
66 baseline artifacts and by replacing the discrete filters on the WVMS instrument with a Fast Fourier
67 Transform (FFT) spectrometer, providing 16,384 channels over a 500 MHz range [Gomez et al.,
68 2012]. Nedoluha et al. [2011] showed that, with an FFT, retrievals had skill down to ~26 km over
69 a five-month period for measurements taken at Table Mountain, California (34.4°N, 242.3°E), and
70 details of the retrieval scheme used here are given therein. The filterbank-based WVMS
71 instrument at Mauna Loa was similarly replaced by a new instrument with an FFT backend in
72 2013, and it is measurements from this instrument that will be shown here.

73 The standard WVMS measurement product is retrieved from a ~1 week integration of the spectrum
74 within +/-30 MHz of the H₂O emission peak at 22 GHz. Results from these retrievals from 1992
75 to 2021 are presented in Nedoluha et al. [2022], where H₂O vertical profiles are shown from 45
76 km to 80 km. Unlike the standard WVMS retrievals, the retrievals for this study make use of a
77 wider +/-160 MHz spectral measurement centered around the H₂O emission peak at 22 GHz with
78 a much shorter integration period. Useful retrievals in the stratosphere can be obtained in ~6 hours
79 of measurement, but the challenge of such measurements in the lower and mid-stratosphere is that
80 the water vapor retrievals are sensitive to very small changes in the instrumental baseline. Making
81 use of 6-hour retrievals minimizes the possibility that a few bad spectral measurements (as can
82 occur, for example, when there is water in the feedhorn antenna) will affect the retrieved water

83 vapor for an entire week. While severely contaminated spectra can be identified and removed
84 from the spectral dataset, even slightly contaminated spectra can cause errors in the retrieved water
85 vapor in the stratosphere.

86 In Figure 1 we show the averaging kernel for a typical WVMS retrieval used in this study. As can
87 be seen, the sensitivity of these 6-hour retrievals drops sharply above ~60 km and they would
88 therefore be inappropriate for mesospheric studies. By comparison, the averaging kernels for the
89 standard weekly retrievals from Mauna Loa show a decrease in sensitivity above ~70 km, and the
90 peak sensitivity at 70 km is ~0.5 [Nedoluha et al., 2022]. It is particularly important for this study
91 to note that the WVMS retrievals, which will be shown down to 28 km, are sensitive to changes
92 in water vapor at altitudes several kilometers below the retrieval altitude.



93
94 **Figure 1-** A typical averaging kernel for a 6-hour WVMS retrieval at Mauna Loa. Each solid line
95 represents the sensitivity of the measurement to a perturbation over a 2 km interval and is
96 referenced to the bottom axis. The dashed line shows the sum of the averaging kernels for these
97 retrievals and is referenced to the top axis. The dot-dashed line shows the sum of the averaging
98 kernels for the standard weekly retrievals.

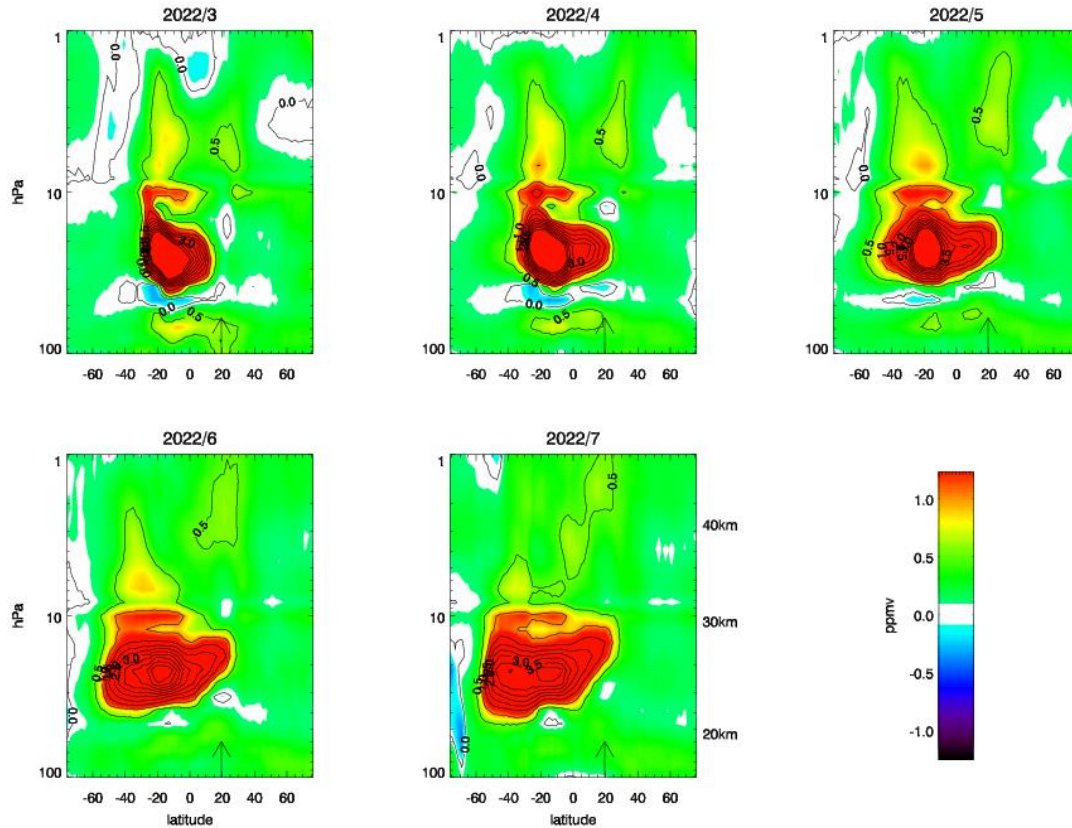
99 3. WVMS and MLS H₂O measurements near Mauna Loa

100 Millan et al. [2022] showed the evolution of the H₂O plume from Hunga Tonga through March
101 2022. The Aura MLS H₂O water vapor product is retrieved from the radiances measured by the
102 radiometers centered near 190 GHz. The v2.2 retrievals were validated by Lambert et al. [2007].
103 The MLS v4 H₂O retrievals were used in Millan et al. [2022] because of poor fits in v5 retrievals
104 in regions of extremely enhanced H₂O. However, Livesey et al. [2021] showed an upward drift in

105 the MLS v4 H₂O measurements of ~2-4%/decade from ~50 hPa to 0.1 hPa since 2010 relative to
106 the Atmospheric Chemistry Experiment Fourier Transform Spectrometer (ACE-FTS) [Bernath, et
107 al., 2005]. Further evidence for this drift is supported by drifts relative to other MLS measurement
108 channels. The MLS v5 retrieval removes the drift relative to ACE-FTS, and the MLS team now
109 generally recommends use of these MLS v5 H₂O retrievals. In addition to the temporal difference
110 between Aura MLS v4 and v5 H₂O retrievals, Aura MLS v5 H₂O is also ~5-10% lower than v4
111 H₂O in the stratosphere and mesosphere. Since the H₂O measurements near Mauna Loa are not as
112 extremely high as was the case near the volcano immediately following the initial eruption, all of
113 the MLS measurements shown here will use the MLS v5 retrieval.

114 In Figure 2 we show the spread of the high water vapor anomaly from Hunga Tonga as observed
115 by MLS from March to July 2022. As is indicated in the figure, the lower stratospheric high water
116 vapor anomaly does not consistently reach the latitude of the WVMS measurements at Mauna Loa
117 until April. The H₂O anomaly also reaches the latitude of the WVMS measurements at Lauder (at
118 45.0°S) in May, but, because of the lower altitude and resultant higher tropospheric optical depth
119 at this site (relative to Mauna Loa and Table Mountain) these measurements do not have the lower
120 stratospheric stability required for a reliable detection. The WVMS measurements at Table
121 Mountain (34.4°N) should be able to detect an increase of this magnitude, but the anomaly does
122 not consistently reach that far north during this time period.

123

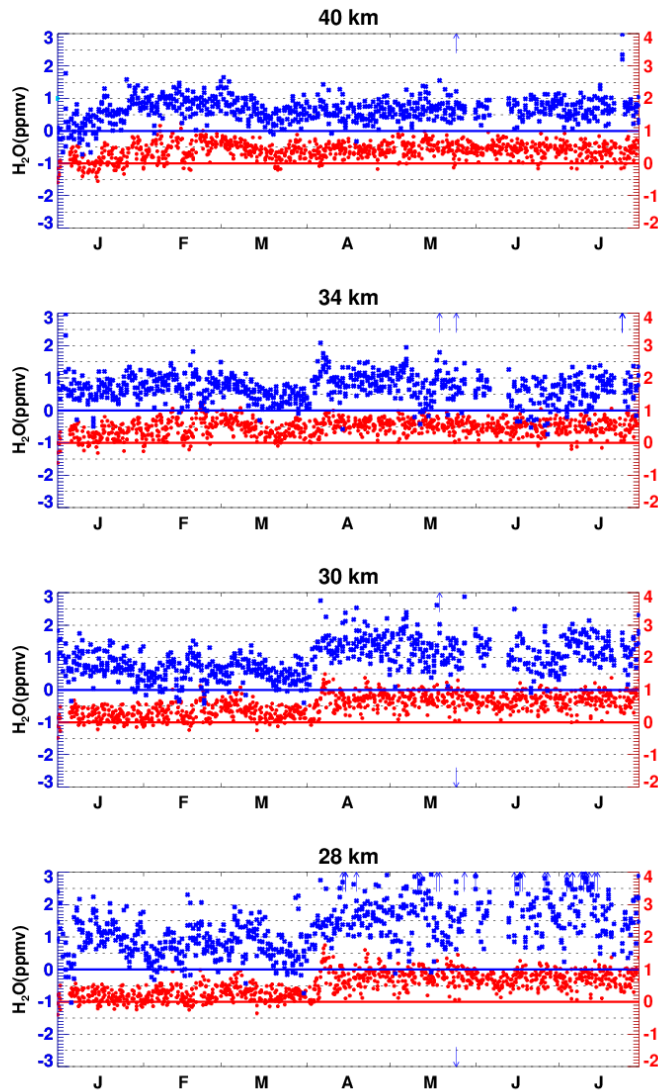


124

125 **Figure 2-** The monthly zonal-median water vapor anomaly relative to the MLS climatology for
 126 MLS measurements from March to July 2022. Data is shown on the native MLS pressure levels.
 127 Indicated altitudes are approximate. The arrow at 19.5N represents the latitude of the Mauna Loa
 128 site.

129 Figure 3 shows water vapor measured by WVMS and Aura MLS (offset by 1 ppmv) near Mauna
 130 Loa in the stratosphere (28, 30, 34, and 40 km) from January through July 2022. As noted above,
 131 WVMS retrievals become increasingly unstable with decreasing altitude in the lower stratosphere,
 132 hence no WVMS retrievals below 28km will be shown here. In Figure 3 the Aura MLS
 133 measurements have been convolved with the WVMS averaging kernels and make use of the same
 134 local MLS-climatology-based a priori (x_{MLS}^{climo}) that is used in the WVMS retrievals, i.e. $x_{sat}^{conv} =$
 135 $x_{MLS}^{climo} + A_{WVMS} \times (x_{sat}^{meas} - x_{MLS}^{climo})$. The measurements up to 34 km show a sudden increase in
 136 water vapor at the beginning of April, with the water remaining elevated from that point onwards.

137



138

139 **Figure 3** – Water vapor retrieval anomalies for January through July 2022 relative to an MLS-
 140 climatology for individual MLS overpasses (red) and 6-hour WVMS measurements (blue). MLS
 141 measurements are within $\pm 2^\circ$ latitude and $\pm 10^\circ$ longitude of Mauna Loa. Note that the y-axes
 142 for the two measurement datasets have been offset by 1ppmv to minimize the over plotting of
 143 points. Arrows indicate individual measurements outside the axis range. The MLS measurements
 144 shown here have been convolved with WVMS averaging kernels.

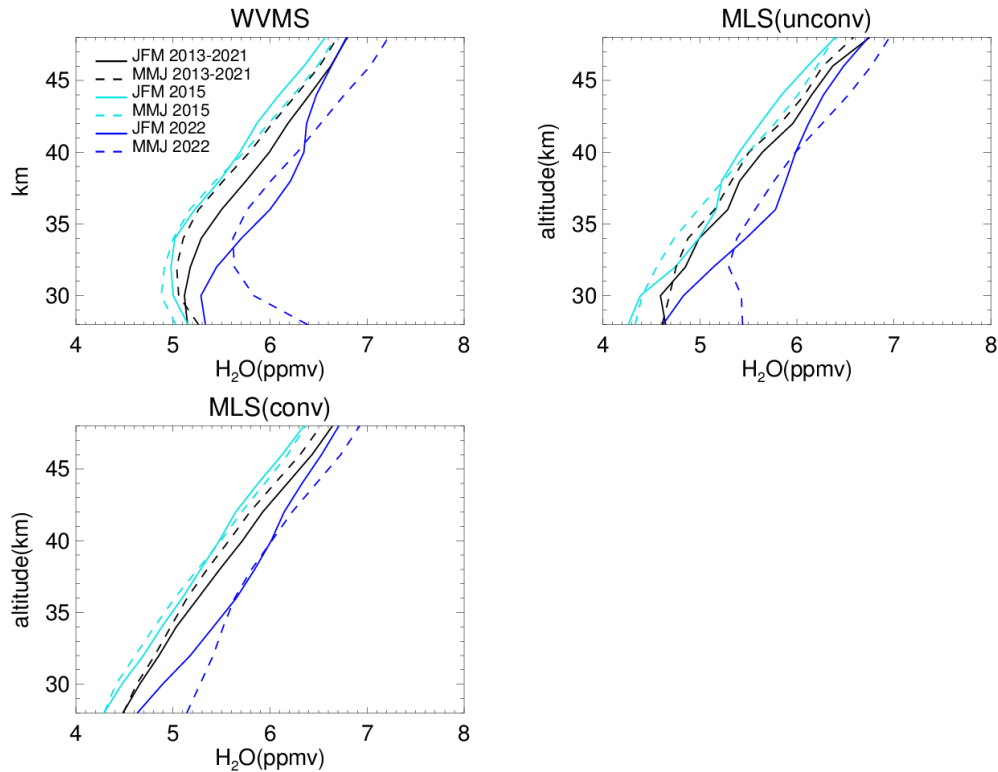
145 In Figure 4 we show stratospheric water vapor profiles measured by the WVMS and MLS
 146 instruments. Each profile shown is either an average of the three monthly profiles for January
 147 through March (JFM), or for May through July (MJJ). For 2022 this separates the three full months
 148 before and after the increase in water vapor when the Hunga Tonga arrived over Mauna Loa.

149 While this study will focus on mixing ratio anomalies, we note that the mixing ratio profiles
 150 measured by the two instruments are generally in good agreement. The exception to this is that
 151 the WVMS H_2O measurements from ~ 28 -34 km do not increase as rapidly with increasing altitude

152 as the MLS measurements. This is probably the result of a small but stable instrumental baseline
153 component in the measurement spectrum in this WVMS instrument which affects the lowest
154 retrieved altitudes. To the extent that this baseline component is stable, it should not significantly
155 affect the retrieved H₂O anomalies.

156 In Figure 4 we show both convolved and unconvolved MLS profiles to help clarify the effects of
157 convolving the MLS profiles to better match the vertical resolution and sensitivity of the WVMS
158 measurements. Surprisingly, the 2022 differences between JFM and MJJ between the WVMS and
159 unconvolved MLS profiles are in better agreement than between the WVMS and convolved MLS
160 profiles. The MLS measurements themselves have a vertical resolution (FWHM of the averaging
161 kernels) of 3-4 km in the altitude range shown [Livesey et al., 2020].

162 To put the 2022 lower stratospheric increase in perspective from a seasonal variation standpoint
163 we also show the 9-year average of the JFM and MJJ profiles for 2013-2021. The average from
164 both instruments shows a decrease in H₂O from JFM to MJJ from 28 to 48 km (with a small
165 exception near ~30 km in the unconvolved MLS profile). Relative to this 9-year average we see
166 that, in addition to the large H₂O increase below ~34 km from the arrival of the Hunga Tonga
167 plume, the H₂O profile in 2022 has several other unusual features. First, we note that in 2022
168 water vapor values are higher than average throughout the stratosphere both before and after the
169 arrival of the plume. Second, we note that the H₂O change from JFM to MJJ is different from that
170 of most years at several altitude levels. In 2022 changes from JFM to MJJ can be separated into
171 three altitude regions. Below ~34 km there is an increase, associated with the arrival of increased
172 H₂O in April. From ~34-40 km there is a smaller decrease in H₂O (similar to what is observed in
173 the 9-year average). And from ~40 km to the stratopause there is again an increase from JFM to
174 MJJ that is not seen in the 9-year average. Note that such a growing positive anomaly is also
175 apparent in Figure 2. Unlike the mid-April increase apparent at 28 km, there is, however, no clear
176 event associated with this increase in upper stratospheric H₂O. The profile for 2015 is also shown
177 in Figure 4 because, as will be discussed later, the Quasi-Biennial Oscillation (QBO) phase of this
178 year is very similar to that of 2022.



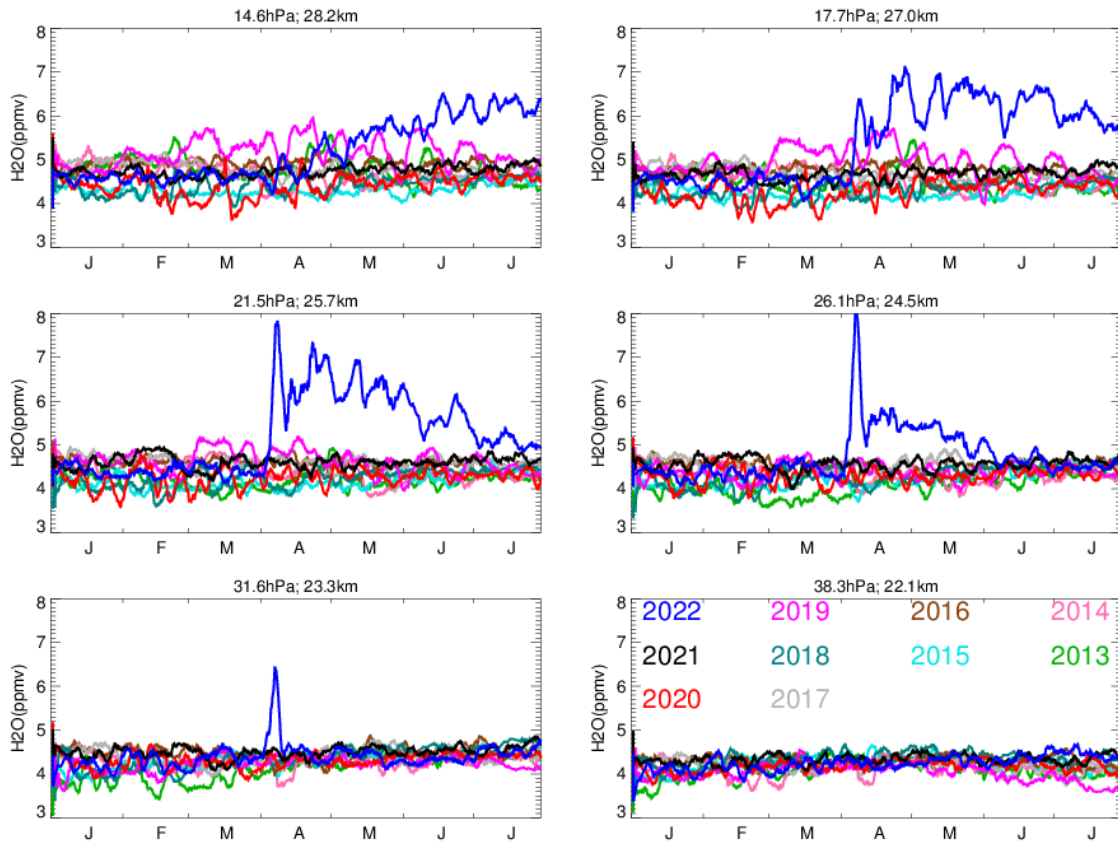
179

180 **Figure 4-** Water vapor profiles over Mauna Loa from WVMS (top left), MLS (top right) and
 181 convolved MLS (bottom left) measurements. Profiles are shown for January-March (solid) and
 182 May-July (dashed), and are separated between a 2013-2021 average (black), 2015 (cyan), and 2022
 183 (blue).

184 In Figure 5 we show MLS measurements in the lower stratosphere from January through July near
 185 Mauna Loa for all years since 2013. The MLS measurements shown in Figure 5 have not been
 186 convolved, and the mixing ratios are shown on the MLS native grid with an approximate altitude
 187 to simplify the comparison with other figures.

188 When compared to the H₂O measured in other years, the increase in H₂O that occurred near Mauna
 189 Loa in April 2022 is clearly an unprecedented event. When the anomaly initially arrived, it was
 190 confined to ~23km to ~27km. In subsequent months in 2022 the H₂O mixing ratio began to rise
 191 at higher altitudes and decrease at the lower altitudes.

192 While the 2022 post-March H₂O from the Hunga Tonga plume is certainly the largest anomaly,
 193 there are other years, especially at the highest level shown in Figure 5 (14 hPa; ~28km) that show
 194 daily mixing ratios that are, throughout these seven months, consistently either higher or lower
 195 than average. As an example, in 2019 the H₂O mixing ratios shown in Figure 5 are consistently
 196 anomalously high. These anomalously high mixing ratios at this level are seen in MLS
 197 measurements throughout the northern hemisphere during this period, and there is no indication
 198 that this was the result of an unusual injection of H₂O. In this study we will attempt to place the
 199 observed stratospheric water vapor increase from Hunga Tonga into the context of these other
 200 interannual variations that have been observed since 2013.



201

202 **Figure 5-** Daily average Aura MLS measurements on the native pressure grid (altitudes are
 203 approximate) from January through July of 2013 through 2022 within $\pm 2^\circ$ latitude and $\pm 10^\circ$
 204 longitude of Mauna Loa.

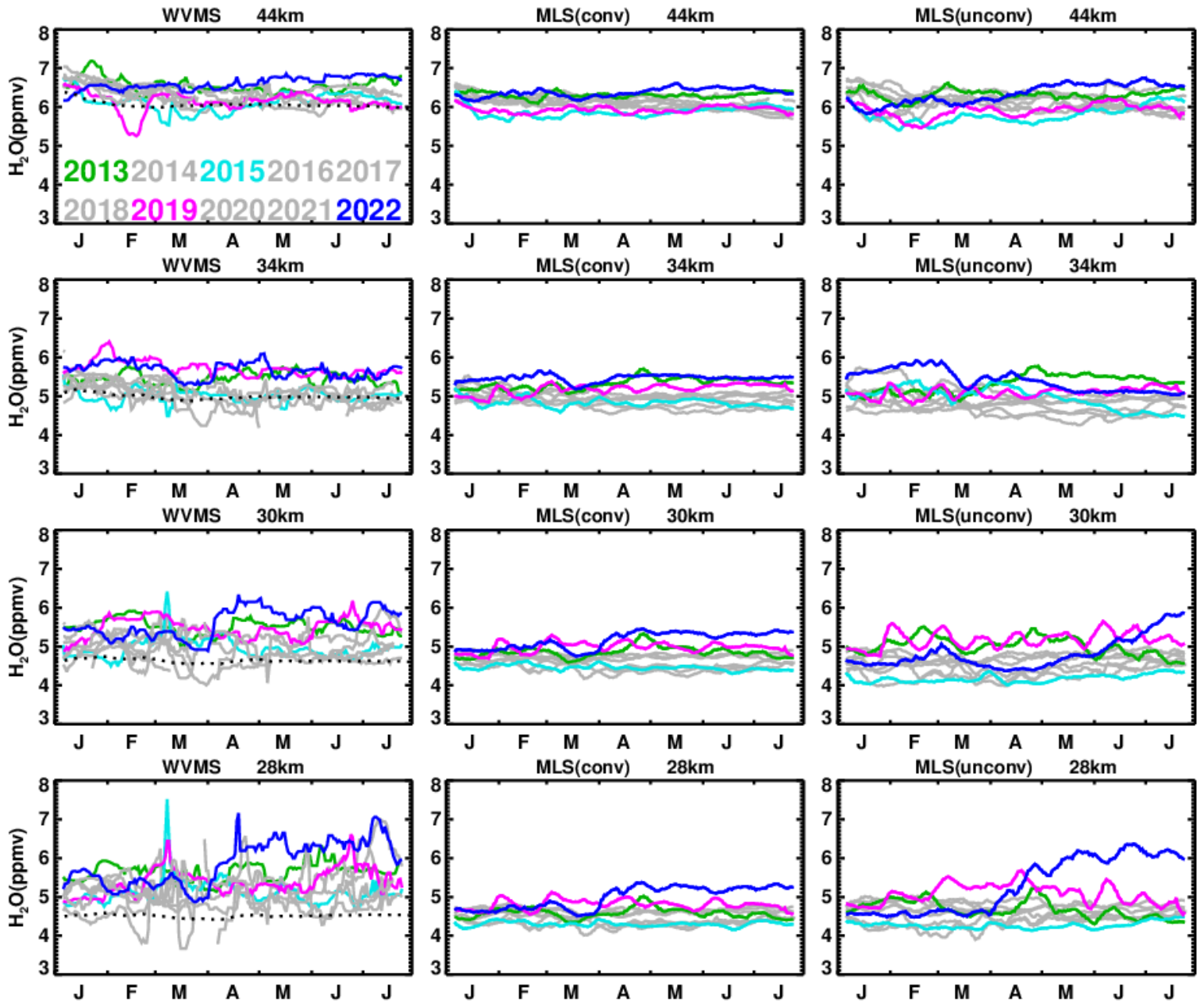
205 In Figure 6 we show a comparison of timeseries for the years since 2013 from both WVMS and
 206 MLS. The WVMS results shown are medians of 6-hour retrievals within ± 5 days of the date
 207 shown. Using medians instead of means minimizes the adverse effect of single retrievals that are
 208 corrupted with baseline artifacts. MLS results are ± 5 day averages and are shown for both
 209 convolved and unconvolved MLS retrievals. The years 2013 and 2019 are highlighted because
 210 these years, along with 2022, show the highest mixing ratios in the mid-stratosphere for much of
 211 the time period shown. Mixing ratios for 2015 are also highlighted, and will be further discussed
 212 below.

213 The WVMS and MLS retrievals at 44 km both show lower than average H_2O throughout most of
 214 the year in 2019, and higher than average H_2O in 2013 and 2022. There is a large drop in the 44km
 215 mixing ratios in February 2019 in the WVMS measurements which shows up with a much smaller
 216 amplitude in the MLS measurements. We think this is probably an instrumental artifact in the
 217 WVMS measurements caused by baseline instability, but we cannot identify a specific
 218 instrumental anomaly.

219 At 34 km the WVMS measured H_2O mixing ratios for 2013, 2019, and 2022 are unusually large
 220 throughout the time period. This differs from the MLS mixing ratios only in that the 2019 MLS

221 mixing ratios are not high in January and February. While the measured mixing ratios are large in
222 January 2022 in all three datasets, there is no indication that this a result of the Hunga Tonga
223 eruption.

224 At 30 km and 28 km the April 2022 increase in mixing ratio begins to stand out as an unusual step
225 increase in the WVMS retrievals. While there are other jumps and drops in mixing ratio of this
226 magnitude in other years (e.g., there is a particularly large spike in early March, 2015 and there
227 are two large temporary dips in February and March 2018), following these events in other years
228 the mixing ratio returns to near its previous level. We assume that these other events are caused
229 by baseline instabilities related to unusual tropospheric conditions, but, besides the unusual mixing
230 ratios, we have no independent evidence that indicates that this data is problematic. What
231 distinguishes the 2022 data is that the mixing ratios remain high following the April increase.

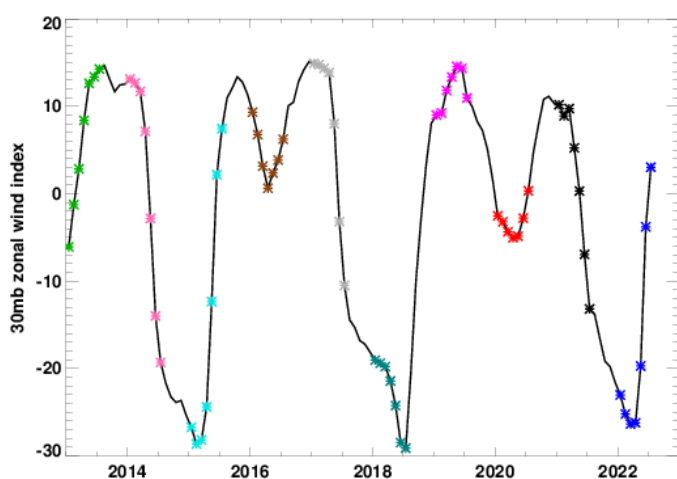


233 **Figure 6-** Water vapor measurements with a +/-5 days smoothing at Mauna Loa from January
 234 through July of 2013 through 2022. Results are shown for WVMS (left column), MLS-convolved
 235 (middle column), and MLS-unconvolved interpolated to WVMS altitudes. Measurements are
 236 highlighted for 2013 (green), 2015 (cyan), 2019 (pink), and 2022 (blue).

237 **4. Other geophysical drivers of interannual variations in stratospheric H₂O**

238 In order to understand the effect of the Hunga Tonga eruption on stratospheric H₂O near Mauna
 239 Loa we investigate other geophysical factors that are known to cause interannual changes in
 240 stratospheric H₂O mixing ratios. Two important factors that drive interannual water vapor

241 anomalies in the tropical stratosphere are the QBO and the average tropical tropopause
242 temperatures. The QBO affects upwelling [Baldwin et al., 2001], which in turn affects dynamics
243 and thus chemical composition [e.g. Schoeberl et al., 2008; Nedoluha et al., 2015]. In Figure 7 we
244 show the 30 mb zonal wind index for each year since 2013. As we noted above, 2013 and 2019
245 had unusually high mid-stratospheric H₂O mixing ratios, and the phase of the QBO is quite similar
246 in 2013 and 2019, having strongly positive zonal wind indices for much of the period shown. This
247 suggests that this phase of the QBO is correlated with the large mid-stratospheric H₂O mixing
248 ratios over Mauna Loa observed during those years. The phase of the QBO in 2022 is, however,
249 not similar to that seen in either 2013 or 2019, but it is similar to that of 2015. Comparisons
250 between 2015 and 2022 can therefore help to determine to what extent unusual H₂O variations in
251 2022 may be related to the phase of the QBO.



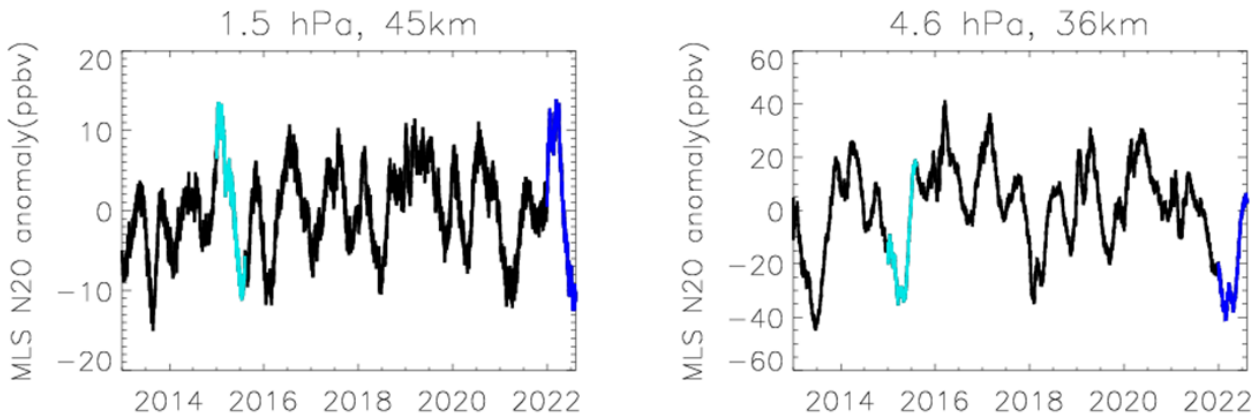
252
253 **Figure 7-** The 30mb monthly zonal wind index from www.cpc.ncep.noaa.gov. The symbols indicate
254 January through July of each year, with the same yearly colors as in Figure 5.

255 An unusual feature that 2015 and 2022 do have in common that is shown in Figure 4 is that,
256 whereas in most years the H₂O mixing ratio in the mid- and upper stratosphere decreases from
257 JFM to MJJ, in 2015 and 2022 there is an increase in mixing ratios above 40 km from JFM to MJJ.
258 The variations in water vapor in the tropical stratosphere are caused both by variations in the
259 amount of water vapor entering the stratosphere from the troposphere, and by dynamical
260 variations. The dynamical variations in H₂O at any particular location are the result of variations
261 in the fraction of CH₄ that has been oxidized. In general, for air parcels ascending unusually slowly
262 (quickly) there is more (less) time for the CH₄ in these unusually old (young) air parcels to oxidize,
263 and hence the H₂O mixing ratio at that particular location will be unusually high (low). Water
264 vapor mixing ratios in the upper stratosphere are particularly sensitive to this dynamical variation.
265 The unusual increasing H₂O from JFM to MJJ in the upper stratosphere above Mauna Loa could
266 therefore be caused by unusual dynamics. If this were the case we would also expect other
267 dynamically sensitive variables to show unusual mixing ratios in this region.

268 While MLS does not measure CH₄, Figure 8 shows that in the upper stratosphere the N₂O anomaly
269 as measured by MLS at 1.46hPa (~45km) is positive in January and negative in July in both 2015

270 and 2022. This indicates that the air over Mauna Loa at 1.46hPa in January is unusually young,
 271 while in July air at this location and pressure level it is unusually old. This is consistent with an
 272 increase in the H₂O anomaly in this region over this period due to the oxidation of CH₄. We
 273 therefore conclude that at least some of the unusual increase in H₂O in the upper stratosphere at
 274 Mauna Loa following that the eruption of Hunga Tonga could be caused by unusual dynamical
 275 variations and not directly by additional H₂O entering the stratosphere. The WVMS and MLS
 276 measurements do both show, however, that the increase in 2022 is somewhat larger than that in
 277 2015, so we cannot completely discount the possibility that some portion of this upper stratospheric
 278 increase in H₂O may be the result of additional H₂O from the eruption.

279 We also show 2015 and 2022 N₂O variations at 4.6 hPa (~36 km) both to emphasize that 2015 and
 280 2022 are dynamically similar at this altitude as well, and to illustrate that at this level a dynamically
 281 driven anomalous increase in H₂O would not be expected. From ~34 km to ~40 km there is a
 282 decrease in H₂O from JFM to MJJ 2022 in the unconvolved MLS measurements, and this decrease
 283 is very similar to that observed in 2015, suggesting that this is a dynamically driven variation. The
 284 WVMS 2022 retrievals show a similar decrease, but only a smaller decrease in 2015, while the
 285 convolved MLS measurements show very little decrease in this range.



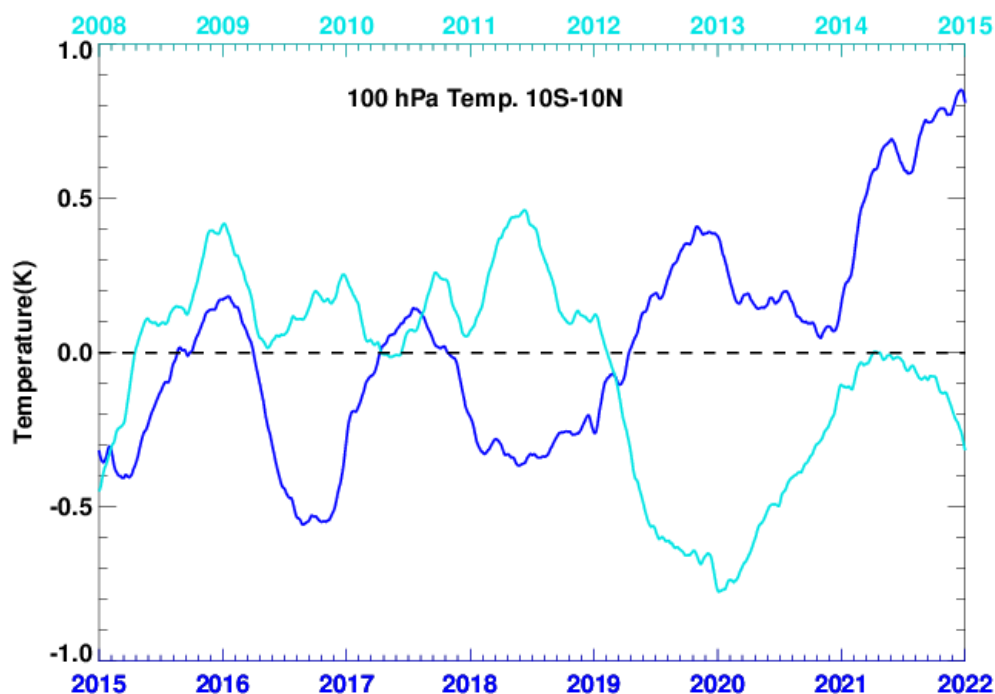
286
 287 **Figure 8-** The anomaly from an MLS climatology for N₂O over Mauna Loa. Results are shown
 288 for 1.46 hPa and 4.6 hPa on the native MLS pressure grid, which corresponds to altitudes of ~45
 289 km and ~36 km. January through July are highlighted for 2015 (cyan) and 2022 (blue).

290 While the phase of the QBO and the associated dynamical anomalies indicated by the N₂O
 291 measurements seem to explain at least some of the unusual upper stratospheric H₂O observed at
 292 Mauna Loa in 2022, there remains the question as to why, even before the Hunga Tonga eruption,
 293 mixing ratios in 2022 up to ~45 km are above average both in JFM and in MJJ, while in 2015 for
 294 those same periods the mixing ratios are below average throughout the stratosphere near Mauna
 295 Loa.

296 As noted above, the other key geophysical factor that affects interannual H₂O variations is tropical
 297 tropopause temperature. The mixing ratio of water vapor that crosses from the troposphere into the
 298 stratosphere is determined by H₂O saturation mixing ratio where the air crosses the cold point
 299 tropopause in the tropics. Seidel and Randel [2006] showed that in the tropics 100 hPa corresponds

300 approximately to the tropopause level pressure, and Tegtmeier et al. [2020] showed in a number
301 of reanalyses (including MERRA2) that changes in 100 hPa temperatures were very similar to
302 those at the cold point level, so in Figure 9 we show tropical (10°S-10°N) temperature anomalies
303 at 100 hPa in the 7 years preceding the beginning of 2015 and 2022 respectively. The temperatures
304 are from MERRA2 and the anomalies are relative to a 1980-present baseline. The precise
305 relationship between cold point tropopause temperature and H₂O saturation mixing ratios (and
306 hence H₂O entering the stratosphere) depends upon the exact temperature and pressure, with
307 Fueglistaler and Haynes [2005] giving a value of ~0.5 ppmv/K, Seidel et al. [2001] ~0.6 ppmv/K,
308 and Nedoluha et al. [1998] ~0.7 ppmv/K.

309 Schoeberl et al. [2005] (their Figure 2) calculated from model spectra that, while the mean age of
310 air at 30km and 18°N is ~3 years, much of the air is much younger, as is clear from the mid-
311 stratospheric measurements of the H₂O plume shown here. We estimate from their figure that
312 ~70% of the air has been in the stratosphere for <3 years. The difference in 100 hPa temperature
313 between 2020-2022 as compared to 2013-2015, or between 2019-2021 as compared to 2012-2014,
314 is ~0.7 K. If we combine this with the sensitivity of saturation mixing ratio to pressure we estimate
315 that the changes in tropical tropopause temperature lead to an increase in stratospheric H₂O over
316 Mauna Loa of ~0.3 to 0.4 ppmv between 2022 and 2015.



317
318 **Figure 9** - Tropical tropopause temperature anomalies from MERRA2 at 100 hPa from 10°S to
319 10°N. Temperatures are shown from the 7 years before 2015 (cyan) and the 7 years before 2022
320 (blue). The data has been smoothed over 365 days and the point at 2022.0 includes temperatures
321 through June 30 2022.

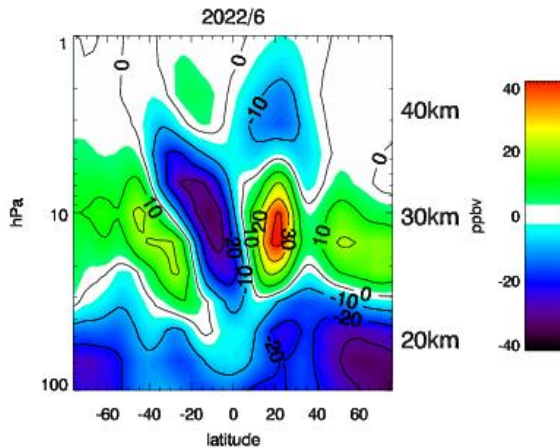
322 Increasing anthropogenic CH₄ emission will also cause some increase in H₂O over this 7-year
323 period. The increase in CH₄ for the 7 years from 2015 to 2021 during this period is ~0.08 ppmv
324 (gml.noaa.gov/ccgg/trends_ch4/) [Lan et al., 2022]. Above the stratopause where CH₄ is fully

325 oxidized each additional CH₄ molecule will produce two H₂O molecules and this would increase
326 H₂O by ~0.15 ppmv. Measurements of CH₄ from HALOE [cf. Remsberg, 2015] show that, in the
327 mid-stratosphere over Mauna Loa, the CH₄ mixing ratio is ~1 ppmv, while at the stratopause it is
328 ~0.3 ppmv. Lan et al. [2022] show that ~1.9 ppmv CH₄ is emitted at the surface, hence ~1/2 of
329 the CH₄ has been oxidized in the mid-stratosphere over Mauna Loa and ~85% at the stratopause,
330 contributing ~0.08 ppmv and ~0.14 ppmv to the observed H₂O increase at these respective
331 altitudes. The average difference of H₂O at 28 km and 48 km in JFM 2022 as compared to JFM
332 2015 is +0.48 ppmv for the WVMS measurements and +0.45 ppmv for the MLS measurements
333 (both convolved and unconvolved), and is therefore approximately consistent with the combined
334 effects of increased tropical tropopause temperatures and increased anthropogenic CH₄ emission.

335 Given that 2015 and 2022 started with very different amounts of stratospheric H₂O over Mauna
336 Loa, we cannot ascribe the high H₂O mixing ratios observed in 2022 entirely to the Hunga Tonga
337 eruption. The similar QBO phases of these two years does, however, lead to similar dynamical
338 changes, and below ~34km there was no increase observed in H₂O during the first seven months
339 of 2015. Hence, there is no reason to suggest that any of the observed H₂O increase at Mauna Loa
340 during 2022 below ~34km to anything other than the Hunga Tonga plume.

341 While we have focused here on changes in H₂O over Mauna Loa, we can apply some of the
342 dynamical conclusions to other latitudes in the tropics. Figure 10 shows the N₂O anomaly for June
343 2022, which looks very similar to that for June 2015. In the upper stratosphere at latitudes near
344 Mauna Loa the negative N₂O anomaly indicates slowly rising air and, as was discussed above, this
345 indicates a region in which more CH₄ oxidation has taken place because the air is unusually old,
346 and hence H₂O will generally be anomalously high. This region is well correlated with the region
347 of increased H₂O shown in Figure 2.

348 In contrast to the upper stratospheric negative N₂O anomaly over Mauna Loa, near 10 hPa the
349 positive N₂O anomaly in the northern tropics indicates that air in this region is rising unusually
350 rapidly, while, in contrast, the air in the southern tropics is rising unusually slowly. This is
351 consistent with Figure 2, which shows that the peak of the water vapor anomaly rises rapidly in
352 the tropics north of the equator, but not south of the equator. While slowly rising air generally
353 results in increased H₂O, in this case the standard photochemically driven anti-correlation between
354 N₂O and H₂O is overwhelmed in the northern tropics by the effect of the rising plume of young
355 and very large H₂O mixing ratio air from Hunga Tonga.



356

357 **Figure 10** – The June zonal-median N₂O anomaly (in ppbv) relative to the MLS climatology for
 358 MLS measurements from 2004-2021.

359 **5. Discussion**

360 As noted by Millan et al. [2022] the eruption of Hunga Tonga at 20.5°S in January 2022 injected
 361 unprecedented amounts of H₂O into the stratosphere. The WVMS measurements at Mauna Loa
 362 (19.5°N) are most accurate and stable in the mesosphere, but, following instrumental
 363 improvements made in 2012, it is possible to usefully retrieve H₂O in the stratosphere as well.
 364 Three months after the Hunga Tonga eruption the WVMS measurements at Mauna Loa observed
 365 a sudden increase at the lowest reliable retrieval altitude 28km. This provided an interesting test
 366 of the ability of the WVMS measurements to retrieve unusual H₂O variations in the stratosphere.

367 Interannual variations in water vapor in the tropical stratosphere are caused by a number of
 368 geophysical factors unrelated to volcanic emissions. Some years show unusually high water vapor
 369 because of dynamical variations related to the QBO. Comparisons between 2015 and 2022 are
 370 particularly instructive because the months from January to July during these years are
 371 dynamically similar in the stratosphere above Mauna Loa. Changes in H₂O caused by dynamical
 372 variations during these months should therefore be similar. However, while dynamical variations
 373 that can cause changes in H₂O are similar in 2015 and 2022, the stratospheric H₂O observed before
 374 the eruption was much higher in 2022. This can be attributed to higher tropical tropopause
 375 temperatures in the previous years, and, to a smaller extent, to increased anthropogenic CH₄
 376 emission over that seven year interval.

377 While H₂O mixing ratios over Mauna Loa in 2022 were already unusually high even before the
 378 arrival of the plume from Hunga Tonga, the sudden increase in H₂O with the arrival of the plume
 379 brought H₂O mixing ratios to even higher levels. The observed increase with the arrival of the
 380 plume brought an unprecedented increase over Mauna Loa that remained present from May
 381 through July. MLS measurements showed that the peak of the mixing ratio ascended during this
 382 period over the northern tropics, but showed much less of an altitude change in the southern tropics.
 383 This change in ascent rate seems to be related to the QBO phase. While much of this study has
 384 been focused on putting the H₂O changes within the context of other geophysically driven
 385 interannual variations in H₂O observed at Mauna Loa, we do emphasize that we only observed the
 386 very northern edge of an H₂O plume that, at the end of July 2022, covered latitudes from ~60°S to

387 20°N. As portions of this plume rise during the next few years it will be of great interest to measure
388 the effect of the eruption on global H₂O at the stratopause and above.

389 **6. Acknowledgments**

390 We thank G. Rose for his efforts to maintain and calibrate the WVMS instrument at Mauna Loa.
391 This work was supported by the NASA Earth Sciences Division Upper Atmosphere Research
392 Program and by the Office of Naval Research. Work at the Jet Propulsion Laboratory, California
393 Institute of Technology, was carried out under a contract with the National Aeronautics and Space
394 Administration. We thank M. Heney for making the daily GMA:GEOS5 temperature data at each
395 site available in a convenient form.

396 **7. Data Availability Statement**

397 WVMS six-hour retrievals (GN2022.SIX.HOURLY) are available on the NDACC data server at
398 www-air.larc.nasa.gov/missions/ndacc/data.html#. MLS v5 data are available at
399 disc.gsfc.nasa.gov/datasets?page=1&keywords=ML2H2O_005. GEOS temperature data are
400 available at gmao.gsfc.nasa.gov/GMAO_products/.

401 **8. References**

- 402 Baldwin et al. (2001), The Quasi-Biennial Oscillation, *Reviews of Geophysics*, 39, 179-229,
403 2001.
- 404 Bernath, P. F., McElroy, C. T., Abrams, M. C., Boone, C. D., Butler, M., Camy-Peyret, C., Carleer, M.,
405 Clerbaux, C., Coheur, P.-F., Colin, R., DeCola, P., DeMazière, M., Drummond, J. R., Dufour,
406 D., Evans, W. F. J., Fast, H., Fussen, D., Gilbert, K., Jennings, D. E., Llewellyn, E. J., Lowe, R.
407 P., Mahieu, E., McConnell, J. C., McHugh, M., McLeod, S. D., Michaud, R., Midwinter, C.,
408 Nassar, R., Nichitiu, F., Nowlan, C., Rinsland, C. P., Rochon, Y. J., Rowlands, N., Semeniuk, K.,
409 Simon, P., Skelton, R., Sloan, J. J., Soucy, M.-A., Strong, K., Tremblay, P., Turnbull, D.,
410 Walker, K. A., Walkty, I., Wardle, D. A., Wehrle, V., Zander, R., and Zou, J.: Atmospheric
411 Chemistry Experiment (ACE): Mission overview (2005), *Geophys. Res. Lett.*, 32, L15S01,
412 <https://doi.org/10.1029/2005GL022386>, 2005.
- 413 Fueglistaler, S., and P. H. Haynes (2005), Control of interannual and longer-term variability of
414 stratospheric water vapor, *J. Geophys. Res.*, 110, D24108, doi:10.1029/2005JD006019.
- 415 Gomez, R. M., G. E. Nedoluha, H. L. Neal, and I. S. McDermid (2012), The fourth-generation
416 Water Vapor Millimeter-Wave Spectrometer, *Radio Sci.*, 47, RS1010,
417 doi:10.1029/2011RS004778.
- 418 Lambert, A., et al. (2007), Validation of the Aura Microwave Limb Sounder stratospheric water
419 vapor and nitrous oxide data products, *J. Geophys. Res.*, 112, D24S36,
420 doi:10.1029/2007JD008724.
- 421 Lan, X., K. W. Thoning, and E. J. Dlugokencky (2022): Trends in globally-averaged CH₄, N₂O,
422 and SF₆ determined from NOAA Global Monitoring Laboratory measurements. Version 2022-
423 09, <https://doi.org/10.15138/P8XG-AA10>

424 Livesey, N. J., et al. (2020), EOS MLS Version 5.0x Level 2 and 3 data quality and description
425 document, Tech. Rep., Jet Propulsion Laboratory, available at: [https://mls.jpl.nasa.gov/eos-aura-](https://mls.jpl.nasa.gov/eos-aura-mls/data-documentation)
426 [mls/data-documentation](https://mls.jpl.nasa.gov/eos-aura-mls/data-documentation).

427 Livesey, N. J., et al. (2021), Investigation and amelioration of long-term instrumental drifts in
428 water vapor and nitrous oxide measurements from the Aura Microwave Limb Sounder (MLS)
429 and their implications for studies of variability and trends, *Atmos. Chem. Phys.*, 21, 15409–
430 15430, 2021.

431 Millán, L., Santee, M. L., Lambert, A., Livesey, N. J., Werner, F., Schwartz, M. J., et al. (2022).
432 The Hunga Tonga-Hunga Ha'apai Hydration of the Stratosphere. *Geophysical Research Letters*,
433 49, e2022GL099381. <https://doi.org/10.1029/2022GL099381>.

434 Nedoluha, G. E., Bevilacqua, R. M., Gomez, R. M., Siskind, D. E., Hicks, B. C., and Russell III,
435 J. M. (1998): Increases in middle atmospheric water vapor as observed by HALOE and the
436 groundbased Water Vapor Millimeter-wave Spectrometer from 1991–1997, *J. Geophys. Res.*,
437 103, 3531–3542, 1998.

438 Nedoluha, G. E., R. M. Gomez, B. C. Hicks, J. Helmboldt, R. M. Bevilacqua, A. Lambert,
439 Ground-based Microwave Measurements of Water Vapor from the mid-Stratosphere to the
440 Mesosphere, *J. Geophys. Res.*, 116, doi:10.1029/2010JD014728, 2011.

441 Nedoluha, G. E., D. E. Siskind, A. Lambert, and C. Boone, The decrease in mid-stratospheric
442 tropical ozone since 1991, *Atmos. Chem. Phys.*, 15, 4215–4224, 2015, doi:10.5194/acp-15-4215-
443 2015.

444 Nedoluha, Gerald E., R. Michael Gomez, Ian Boyd, Helen Neal, Douglas R. Allen, David
445 Siskind, Alyn Lambert, and Nathaniel J. Livesey, Measurements of Mesospheric Water Vapor
446 from 1992 to 2021 at three stations from the Network for the Detection of Atmospheric
447 Composition Change, *J. Geophys. Res.*, in revision 2022.

448 Remsberg, E. E., Methane as a diagnostic tracer of changes in the Brewer–Dobson circulation of
449 the stratosphere, *Atmos. Chem. Phys.*, 15, 3739–3754, 2015, doi:10.5194/acp-15-3739-2015.

450 Schoeberl, M. R., A. R. Douglass, B. Polansky, C. Boone, K. A. Walker, and P. Bernath (2005),
451 Estimation of stratospheric age spectrum from chemical tracers, *J. Geophys. Res.*, 110, D21303,
452 doi:10.1029/2005JD006125.

453 Schoeberl, M. R., et al. (2008), QBO and annual cycle variations in tropical lower stratosphere
454 trace gases from HALOE and Aura MLS observations, *J. Geophys. Res.*, 113, D05301,
455 doi:10.1029/2007JD008678.

456 Seidel, D. J., R. J. Ross, J. K. Angell, and G. C. Reid (2001), Climatological characteristics of
457 the tropical tropopause as revealed by radiosondes, *J. Geophys. Res.*, 106, D8, 7857-7878, 2001.

458 Seidel, D. J., and W. J. Randel (2006), Variability and trends in the global tropopause estimated
459 from radiosonde data, *J. Geophys. Res.*, 111, D21101, doi:10.1029/2006JD007363.

460 Tegtmeier, S., et al. (2020), Temperature and tropopause characteristics from reanalyses data in
461 the tropical tropopause layer, *Atmos. Chem. Phys.*, 20, 753–770, 2020.